CERNE

Characterization of raw and thermochemically-treated mesocarp fibers of *Oenocarpus bataua*, an Amazon palm

Orimax Monteiro Cruz[1][iD], Matheus Cordazzo Dias[2][iD], Dhimitrius Neves Paraguassú Smith de Oliveira[3][iD],
Marcela Gomes da Silva[3][iD], Tiago Marcolino de Souza[2][iD], Lourival Marin Mendes[4][iD],
Lays Camila Matos[3][iD], Lina Bufalino[3]❖[iD]

[1]Federal University of Amapá, Brazil
[2]University of Amapá State, Brazil
[3]Rural Federal University of Amazonia, Brazil
[4]Federal University of Lavras, Brazil

TECHNOLOGY OF FOREST PRODUCTS

ABSTRACT

Background: Patauá (*Oenocarpus bataua* Mart.) is a palm tree belonging to the botanical family Arecaceae that occurs throughout the Amazon. Like açaí, an edible pulp is extracted from its fruits, remaining a fiber-rich waste. Revealing the potential of such raw or thermochemically modified fibers for producing bioproducts is a novelty in the literature. Therefore, this work aimed to characterize patauá fibers in natural and alkali-treated conditions to support future bioproduct applications. Alkaline treatments were performed under mechanical stirring combining two NaOH levels (5 and 10%) and two temperatures (80 and 100°C). Morphological characterization was performed by light microscopy and scanning electron microscopy (SEM). The contents of the structural and non-structural chemical components were determined, and chemical groups were evaluated by Fourier-transform infrared spectroscopy (FTIR). The physical characterization included moisture content, apparent density, and water absorption tests.

Results: The macerate revealed short fibers with typical elongated morphology, mean cell wall thickness (4.10 μm) greater than the mean lumen width (3.01 μm), and mean length of 445 μm. The alkaline treatments partially individualized the fibers from bundles, cleaned extractives from the surface, and unblocked superficial pits by removing silica-rich structures. They substantially removed non-cellulosic components, but FTIR showed condensed lignin exposed on the fiber surface. Density and water uptake increased concerning natural fibers. Patauá's short length and susceptibility to modification through thermochemical treatments that concentrated cellulose up to 50% indicated great potential for developing composites and nanofibers. Regardless of the NaOH content, 100°C was more efficient in concentrating cellulose.

Conclusion: Patauá fibers have unique natural characteristics. They occur as flatted fiber bundles, have silicon-rich structures obstructing their superficial pits, and comprise more lignin than cellulose.

Key words: fiber morphology; lignocellulosic; chemical composition; patauá; mercerization

HIGHLIGHTS

This work brings the first detailed characterization of Patauá mesocarp fibers.
Short thick-walled fiber cells compose flat bundles covering the patauá seeds .
Alkali treatments removed amorphous components and raised cellulose up to 50%.
Mercerization enhanced fiber morphology and density for composite applications.

INTRODUCTION

The Amazon is the largest tropical forest in the world, with several natural resources to support the region's socioeconomic development. It holds the largest biodiversity reserve on the planet, which is little explored concerning its enormous biotechnological potential. Therefore, it is essential to transform these resources into sustainable products without causing environmental damage (Gross, 2016). Palm trees belong to Arecaceae, one of the most representative plant families in the tropical region. It is an easily recognizable group that composes the natural landscape and has great ecological and economic importance. Additionally, palms provide several raw materials for developing non-timber forest products (NTFPs), widely used by the local population for feeding purposes, covering and building houses, ornamentation, and others (Henderson, 1995).

Patauá (*Oenocarpus bataua* Mart.) is a palm tree belonging to the botanical family Arecaceae that occurs throughout the Amazon (Henderson et al., 1995). The name of the patauá genus is an allusion to its more traditional use in Lattin, its fruit pulp; hence *oinos* (Oeno) = wine, and *karpos* (*carpus*) = fruit (Balick, 1986). After noticing its juice, naturalists named the species over two centuries ago (Balick, 1988). In times of açaí off-season, Pará communities consider patauá a substitute food. The patauá pulping generates a waste composed of a seed covered by surficial fibers of lignocellulosic nature with the potential for developing bioproducts (Cruz et al., 2019).

Studies with natural fibers increased in the early 1990s due to the requirements of legislative authorities regarding the use and destination of synthetic fibers and resins derived from petroleum, as well as greater consumer awareness of preserving the environment (Silva, 2003). Thus, one of the potential uses of residual natural fibers is their destination for the production of various biomaterials, such as paper (Jin et al., 2022), cellulose nanofibers (Braga et al., 2021), biocomposites (Ghalehno et al., 2020) and energy (Bufalino et al., 2018).

Currently, the use of agroforestry residues to produce biomaterials is a relevant topic. Plant fibers are cellulose-rich, low-density, economical, widely available, biodegradable, non-abrasive, and non-toxic. However, the lack of good interfacial adhesion between fibers and matrix and its hydrophilicity are drawbacks for their application as composite reinforcements. Removing most non-cellulosic components to produce cellulose nanofibrils without damaging the fiber morphology is important. Surface treatments to modify the fiber's morphological and chemical characteristics can overcome some limitations hindering fiber applications and conversion into engineering materials (Oliveira et al., 2019). Previously to composite production, the thermochemical alkaline treatments or mercerization modifies the fiber surface to improve bonding between the fibers and the polymer matrix (Simelane and Madyira, 2023). As pretreatment for later nanofibrillation and production of nanostructured films, it concentrates cellulose and loosens microfibrils for proper shearing (Fonseca et al., 2019).

A previous study reported that an alkaline treatment with 5% NaOH at 80°C partially individualized patauá fibers from the natural bundles, increased their crystallinity index, and partially cleaned surface impurities (Cruz et al., 2019). Nevertheless, some applications require higher degrees of fiber modification demanding new studies to explore other parameter combinations for the patauá fibers' thermochemical treatments. For instance, biocomposites demand effective cleaning of fiber surfaces for better interface-matrix compatibility without damaging morphology or excessively raising water uptake. Future production of cellulose nanofibrils demands cellulose concentration and microfibrils release.

In addition, as a little-known fiber, literature studies on the complete chemical characterization (extractives, ashes, cellulose, hemicellulose, and lignin) and biometry of patauá fibers are unavailable. Previous work with the açaí fibers, also composing a palm mesocarp, showed varied levels of modification by combining different NaOH concentrations and stirring temperatures (Oliveira et al., 2019), raising interest for a similar study with patauá fibers. Therefore, this work aimed to characterize patauá fibers in natural and alkali-treated conditions to support future bioproduct applications.

MATERIAL AND METHODS

Raw material description and alkaline thermochemical treatments

The patauá fruit was collected in January 2021 in the municipality of Afuá, Pará state, northern Brazil, at a south latitude of 00°09"12" and a west longitude of 50°23'12". The waste from processing the patauá fruits was obtained from local pulping machines, known as "beaters," in Macapá, Amapá, northern Brazil. The washing of the post-processing residue was carried out in distilled water. The removal of fibers from patauá seeds was carried out manually. Before the thermochemical treatments, fibers were immersed in distilled water in a 10 g/L proportion for 24 h for saturation and volume reduction. Two temperatures (80 and 100°C) and two concentrations (5 and 10%) of sodium hydroxide (NaOH) were combined into four thermochemical treatments. Treated fibers were compared to raw fibers. A ratio of 10 g/L of previously saturated fibers was used for each thermochemical modification. Previously, the aqueous NaOH solutions were heated to the target temperatures (80 or 100°C) using a heater stirrer, and the temperature was controlled using a thermometer. Afterward, the fibers were immersed in the solutions and kept under mechanical agitation for 1 h. Then, the samples were washed with running water until neutral pH. Figure 1 illustrates the fruit, fiber-containing waste, separated fibers and seed, and thermochemically treated fibers.

Figure 1: From the fruit to the thermochemically treated patauá fibers: (a) fruit brunch; (b) harvested fruits; (c) de-pulped seed waste (left) and fruit (right); (d) raw fibers (left) removed from the surface of the seeds (right); (e) raw fibers (left) and fibers treated with 10% of NaOH at 100°C.

Morphological characterization

Light microscopy and fiber biometry

The maceration of the natural fibers was carried out, which consists of the individualization of the cells by dissolving the middle lamella (Franklin, 1945). The images of the temporary slides were taken with a Motic optical microscope (BA310Elite). Fiber length, fiber width, lumen width, and wall thickness were measured using the Motic Image Plus 3.0 program. Sixty fibers were measured according to the standard of the International Association of Wood Anatomists (IAWA, 1989).

Scanning electron microscopy (SEM)

SEM was performed to observe if the thermochemical treatments individualized the fibers from the bundles and cleaned the amorphous superficial incrustations and the superficial pits. The samples of all treatments were spread over double-faced carbon adhesive tapes, previously glued onto the aluminum sample holder (stubs). SEM micrographs were obtained using a JMS 6510 scanning electron microscope (JEOL®) with a voltage of 10 kV.

Chemical characterization

Contents of structural and non-structural components

The fibers were cut into a length of ≈ 1 mm and sieved to eliminate those above 18 mesh. Analyses of extractives, ash, soluble lignin, insoluble lignin, holocellulose, and cellulose were performed in triplicate. For total extractives content analysis, the samples underwent extraction in Soxhlet extractors following the T204 cm-17 standard (TAPPI, 2017) soluble in toluene/ethanol (1:1 v/v, 8 h), ethanol (8 h) and boiling water (2 h). The incineration method provided the ash content following the T413 om-17 standard (TAPPI, 2016). The Insoluble lignin content analysis was determined according to the procedures described in the T222 om-15 standard (TAPPI, 2015). The soluble lignin content was determined following the procedures of the UM 250 standard (TAPPI, 2000). Samples of the filtrates resulting from the determination of insoluble lignin were transferred to a quartz cuvette and analyzed in a UV-VIS - M51 model spectrometer from Bel equipment. The absorbance readings of the samples were performed at the wavelengths of 215 nm and 280 nm. The soluble lignin content was determined using [eq. 1]. Where: *LS* = soluble lignin content; *A215* = absorbance at 215 nm; *A280* = absorbance at 280 nm; *mi* = initial mass of fibers (g).

$$LS = (\frac{(4,538 \times A_{215}) - A_{280}}{300 \times mi}) * 100\% \tag{1}$$

The methodology described by Browning (1967) was followed to determine the holocellulose of the extractive-free samples. The cellulose content was obtained following the Kennedy et al. (1987) methodology using the holocellulose samples of the previous analysis.

Fourier Transform Infrared Spectroscopy (FTIR)

Spectroscopy measurements in the Infrared Region were performed to verify if the thermochemical treatments promoted changes in the functional chemical groups of the fibers. A Fourier Transform Infrared Spectrophotometer Perkin Elmer Spectrometer (Frontier) in Total Attenuated Reflection (ATR) mode, from 4000 to 650 cm⁻¹, with 32 scans and a resolution of 4 cm⁻¹, was used in our analysis.

Physical characterization

Physical analyses were performed in triplicate. Dry-basis moisture content was determined according to NBR 14929 (ABNT, 2017). Samples of approximately 1 g were weighed and dried in an oven at 103ºC (±2ºC) until the material mass stabilized with a maximum variation of 0.5 g. Apparent density was obtained according to MB 1269 (ABNT, 2003). The mass was first obtained on a scale with a precision of 0.001 g and volume by immersion in a 10 mL beaker containing alcohol. The volume unit was adjusted to cm³ based on the alcohol's specific mass. The apparent density was determined by the ratio between the mass and volume of the material in the dry base moisture content described above. Water absorption analysis was based on NBR NM 30 (ABNT, 2001). Samples were immersed in water and weighed at 0.001 g precision after 5, 15, and 30 min, and then after 1, 24, 48, and 72 h.

RESULTS

Anatomy and morphological modifications of patauá fibers

The maceration properly individualized the patauá bundles into individual fibers that showed a typical elongated morphology with a closed end and lumen (Figure 2).
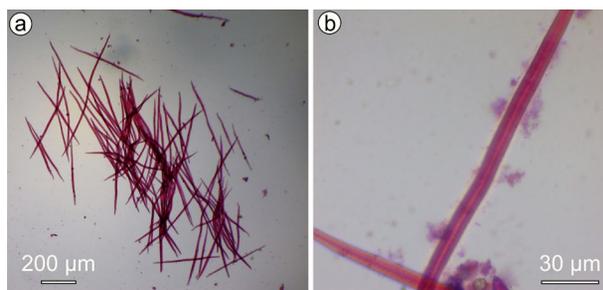
Figure 2: Optical micrographs of macerated patauá fibers: (a) general view, and (b) lumen and cell wall.

Fiber biometry revealed a length/mean thickness ratio of ≈ 40, in addition to a cell wall with a mean thickness greater (4.10 μm) than the mean lumen width (3.01 μm). Based on the coefficient of variation, the most variable property was lumen width, followed by fiber length, wall thickness, and fiber width (Table 1).

Table 1: Descriptive statistics of the biometric variables of patauá fibers.

Biometric parameter	Average (μm)	Coefficient of variation (%)
Fiber length	444.66	25
Fiber width	11.21	16
Lumen width	3.01	30
Wall thickness	4.10	18

SEM showed that the morphology of the fibers changed substantially after alkaline treatment. Untreated fibers have a more rigid structure and larger diameters. After treatment, the fibers partially individualize, consequently reducing the diameter of the treated fibers. Besides, they become softer, with a cleaner and rougher surface. Additionally, a new feature was evident that did not appear in the macerate. The bundles of fibers from the partial individualization are not typically cylindrical but flattened. Another remarkable trait of the raw fibers concerns structures that obstruct the superficial pits. Milder treatments partially removed those structures, while the strongest one (10% of NaOH at 100°C) opened all pits (Figure 3).

Chemical modifications of patauá fibers

Alkaline thermochemical treatments modified the chemical composition of patauá fibers. The effect on the extractive content was variable, with a notable reduction in the most intense treatment (NaOH 10% and 100°C). Ash levels of all treatments were raised regarding the raw control fibers. There was a decrease of up to 4% in all treatments' insoluble and soluble lignin contents. The removal of hemicelluloses was very effective and proportional to the intensity of the treatments. An increased concentration of cellulose accompanied this reduction. It is remarkable that, regardless of the NaOH content, 100°C was much more efficient in the cellulose concentration than 80°C (Table 2).

The FTIR spectra of the different treatments varied concerning the raw fibers. The peak at around 3390 cm^{-1} flattened for the fibers treated at 5% and 80°C but sharpened for the other treatments. The peak at 2975 cm^{-1} increased for patauá fibers treated with NaOH at 5% and decreased for those treated with NaOH at 10%, regardless of the temperature. The peak at 1658 cm^{-1} shifted and flatted for the 5% at 80°C-treated patauá fibers and slightly reduced for the other treatments. The peaks at 1527 cm^{-1}, 1485°C, and 1186 cm^{-1} were absent or weak in the raw fibers and markedly increased after all treatments. The height of the peak at 1048 cm^{-1} decreased for all treatments, especially for the one carried out with NaOH at 5% and 80°C. No remarkable differences occurred among treatments for the peaks at 2891 cm^{-1} and 878 cm^{-1} (Figure 4).

Modifications of the physical properties of patauá fibers

Figure 5 shows the moisture content of the fibers ranging from 9.51 for natural fibers to 12.63% for fibers treated at 10% at 80° C. Concerning bulk density, low variations occurred among fibers treated with different temperatures and NaOH percentages. However, compared to untreated fibers, they were all higher.

The water absorption of the Patauá fibers under all conditions sharply increased up to 1 h and softly continued to increase from 24 to 72 h. All treatments remarkably raised the water uptake, especially those carried out at 100°C. The fibers treated with NaOH level of 10% and 100°C had the highest absorption. Most absorptions surpassed 100% of the fiber mass (Figure 6).
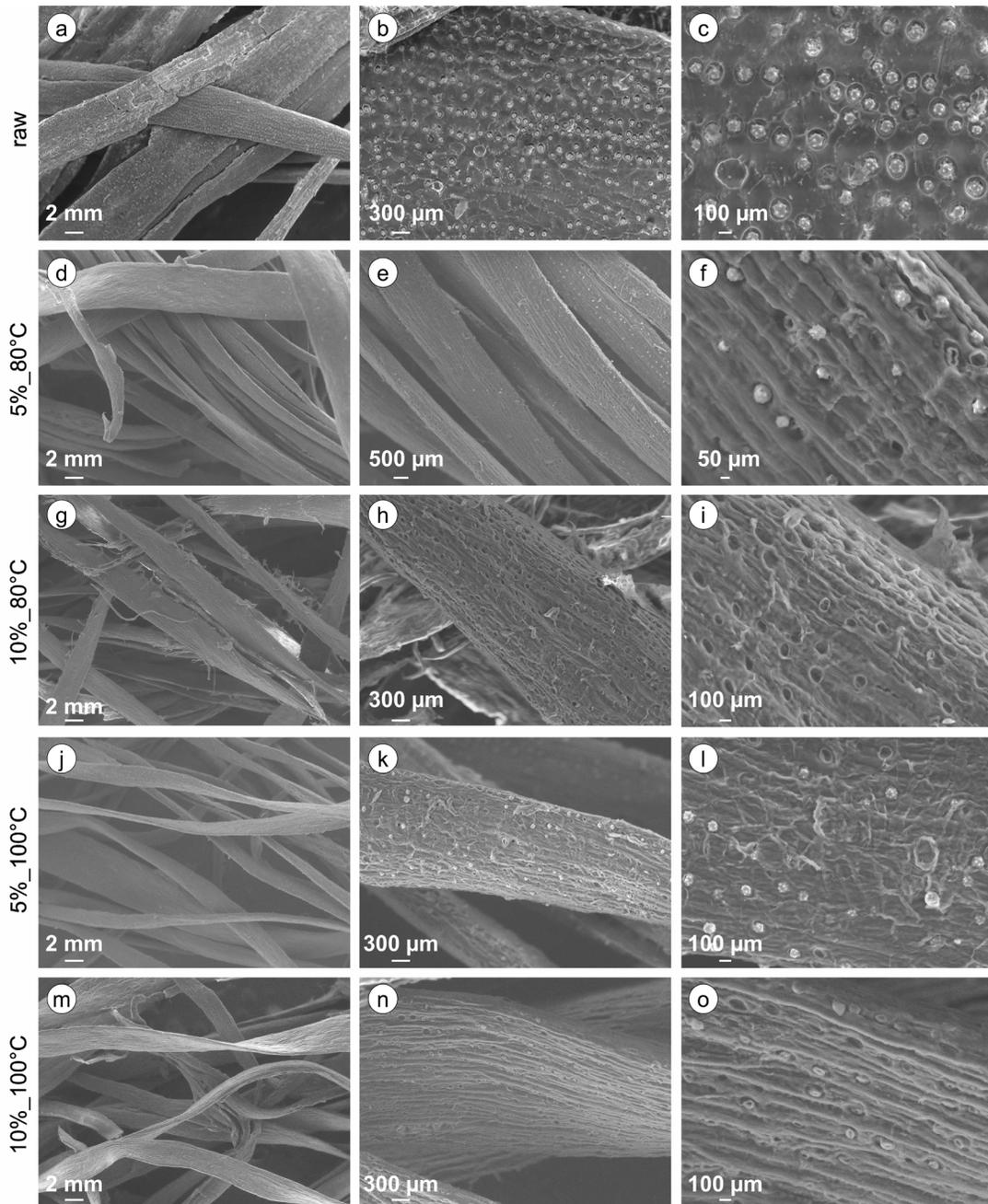
Figure 3: SEM micrographs of the patauá fibers: (a-c) raw, (d-f) treated with NaOH at 5% at 80°C, (g-i) treated with NaOH at 10% at 80°C, (j-l) treated with NaOH at 5% at 100°C, and (m-o) treated with NaOH at 10% at 100°C.

Table 2: Chemical composition of the patauá fibers: raw, treated with NaOH at 5% at 80°C, treated with NaOH at 10% at 80°C, treated with NaOH at 5% at 100°C and treated with NaOH at 10% at 100°C.

Level (%)	Raw	5%_80°C	5%_100°C	10%_80°C	10%_100°C
Extractives	4.8 ± 0.1	6.3 ± 0.2	3.6 ± 0.3	4.4 ± 0.2	2.1 ± 0.1
Ashes	1.1 ± 0.1	2.1 ± 0.1	2.2 ± 0.1	2.9 ± 0.1	2.6 ± 0.8
Insoluble lignin	34.8 ± 2.0	29.6 ± 0.4	30.6 ± 0.5	30.1 ± 2.0	31.0 ± 0.8
Soluble lignin	3.7 ± 0.1	2.8 ± 0.4	2.6 ± 0.1	3.2 ± 0.2	2.7 ± 0.1
Hemicelluloses	34.2 ± 0.3	25.2 ± 0.8	19.1 ± 1.1	20.7 ± 1.2	16.1 ± 0.0
Cellulose	24.3 ± 1.0	37.7 ± 0.8	48.1 ± 1.1	41.3 ± 1.8	48.4 ± 1.3
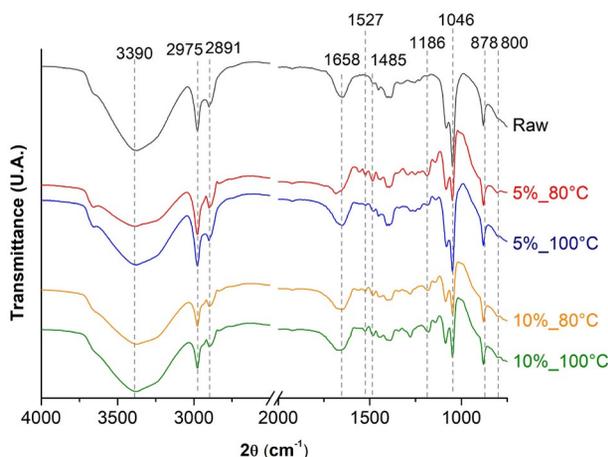
Figure 4: FTIR spectra of the patauá fibers: raw, treated with NaOH at 5% at 80°C treated with NaOH at 10% at 80°C, treated with NaOH at 5% at 100°C, and treated with NaOH at 10% at 100°C.
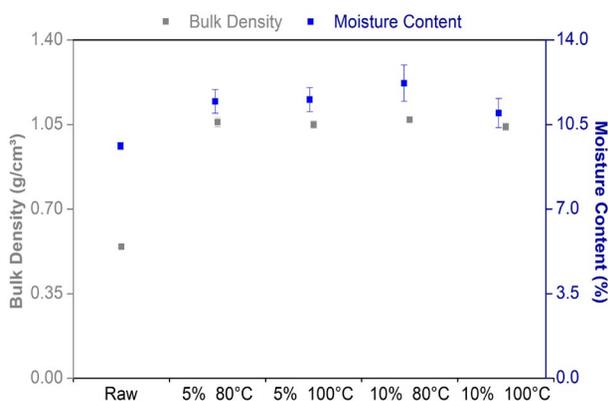
Figure 5: Bulk density and moisture content of the patauá fibers: raw, treated with NaOH at 5% at 80°C, treated with NaOH at 10% at 80°C, treated with NaOH at 5% at 100°C, and treated with NaOH at 10% at 100°C.
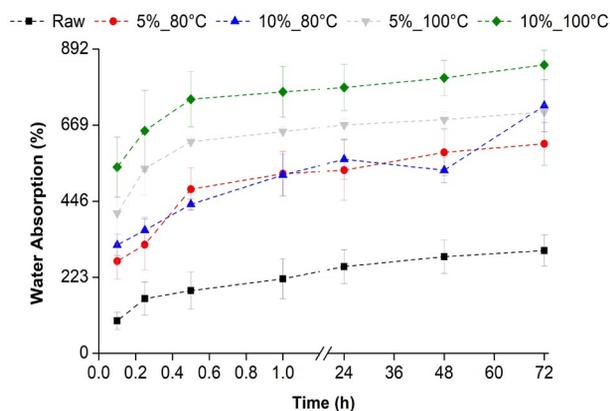
Figure 6: Water absorption of the patauá fibers over time: raw, treated with NaOH at 5% at 80°C, treated with NaOH at 10% at 80°C, treated with NaOH at 5% at 100°C, and treated with NaOH at 10% at 100°C.

DISCUSSION

The biometry of fibers directly affects their applications for bioproducts, including paper, cellulose nanofibers and nanostructured films, and biocomposites. Therefore, comparing the patauá fiber biometry with the most used natural fibers provides useful insights into its potential. A study showed *Pinus glabra* pulp comprising tracheids with a length of 3.14 mm, a width of 27.18 µm, a lumen diameter of 15.39 µm, a wall thickness of 5.89 µm, and a length/diameter ratio of 166 (Vivian et al., 2020). Meanwhile, the macerate of *Eucalyptus camaldulensis* had fibers with a length of 0.86 mm and a length/diameter ratio of 47 (Hassan et al., 2020). The patauá fiber in this study, perfectly isolated by maceration, had a length of 0.23 to 0.73 mm. Therefore, patauá waste is a non-timber raw material that, if subjected to pulping, would provide fibers with similar lengths to eucalyptus pulp. Regarding fiber wall thickness, patauá fibers are classified as thick-walled, with the fiber lumen less than three times double the cell wall thickness (Wheeler et al., 1991). Patauá fiber showed a cell wall thicker than the lumen and a lower length/diameter ratio than wood structures, fibers and tracheids (Vivian et al., 2020; Hassan et al., 2020).

The patauá fiber biometry supports some predictions on its behavior on the future development of bioproducts. Compared to continuous or long fibers, the advantage of short fibers, combined with thermoplastic polymers, is their processability (Junaedi et al., 2020). Their ease of adhesion and dispersion may enhance the flexural strength of composites (Babé et al., 2020). Moreover, a small lumen size means increased wall thickness and loadbearing capacity (NagarajaGanesh and Rekha, 2020). Regarding nanostructured cellulose films, those derived from short fibers may present a higher Young modulus but lower tensile strength than those of longer fibers (Fonseca et al., 2019). As an extra advantage, they are fibers that are weakly adhered to the surface of seeds and removable by hand (Morais et al., 2019), unlike wood fibers that require high pressure and temperature for pulping.

SEM revealed the patauá fibers naturally occur in a bundle shape similar to non-wood fibers such as açaí (Oliveira et al., 2019) and *Stipa tenacissima* – Alfa plant (Ajouguim, 2018). After alkaline treatments, the fibers would have morphology and diameter size close to those of the macerate If a full individualization of the adjacent fibers had occurred. After all treatments, the structures' flattened morphology and diameter of about 2 mm (greater than macerate's) indicate partial fiber individualization. Nevertheless, natural fibers were thicker than the treated ones. Removing lignin and hemicelluloses, the natural binder among cellulose fibers and microfibrils within the cell wall, justifies fiber bundle deconstruction (Benini, 2015), and even microfibrillation can occur (Mulinari, 2014).

When alkali treatment eliminates a substantial amount of amorphous components while preserving the fiber backbone structure and integrity, the surface becomes fibrillated, supporting compatibility with synthetic polymers and improving fiber/polymer interfacial adhesion (Nassar et

al., 2022). Partial individualization from fiber bundles with milder alkali treatments and complete individualization with stronger treatments were also observed for jute (Fonseca et al., 2019) and açaí (Oliveira et al., 2019) fibers.

From the mildest (5% at 80°C) to the strongest (10% to 100%) treatments, the efficiency of removing superficial pit-obstructing structures increased. Previous work with the açaí pulping waste, also composed of fiber-covered seeds, showed similar granulated spherical structures in the fiber surface. Authors proved they are silica-rich and, as observed herein, partially or completely removable from the surface depending on the intensity of the alkaline treatments (Oliveira et al., 2019). Such empty pits could improve composite fiber-matrix interaction through resin flowing toward the fiber lumen.

The efficient removal of extractives explains the fiber "cleaning" and increase in cell wall roughness (Oliveira et al., 2019). These modifications are advantageous for producing composites by improving the interfacial adhesion between fiber and matrix (Zakikhani et al., 2014; Bousfield et al., 2018; Noori et al., 2021; Nassar et al., 2022). Regarding the levels of the non-structural organic extractives and ashes, their increase with the alkali treatments requires careful analysis. Extractives comprise a biomass fraction of organic molecules, such as fat, wax, and others. They are leachable by organic solvents (Attard et al., 2020; Ajouguim et al., 2018). They appear on the fiber surface as many layer incrustations (Ajouguim et al., 2018). SEM confirmed the removal of both inorganic fractions corresponding to the silica-rich structures (Mabrouk et al., 2012) and extractives. Therefore, NaOH treatment residue is the only plausible explanation for the raises in extractives and ashes.

The primary chemical composition of plant fibers is of major relevance for their applications. A paper reported cellulose, lignin, and hemicellulose levels from 45-50%, 21-27%, and 21-31% for Yellow Birch hardwood and Pine softwood. In contrast, cotton depicted over 90% of cellulose and less than 2% of lignin, while 37% of cellulose and 40% lignin comprised coir fibers (Hassan et al., 2020). Therefore, it is noticeable that the mentioned non-wood materials had higher cellulose content and lower lignin content than patauá raw fibers.

Depending on the desired bioproduct, such lignin-richness can be a drawback or an advantage. It can hinder further nanofibrillation (Lönnberg et al., 2016) and harm the composite's fiber-matrix interface (Noori et al., 2021). On the other hand, lignin improves the composites' hydrophobicity and water-repelling ability (Li et al., 2021); hence, excessive removal is not ideal. Although minor, the removal of soluble and insoluble lignin through all treatments was unexpected. Eventually, mercerization does not remove at all or even increases lignin content because of the relative removal of other components (Noori et al., 2021). Therefore, patauá fibers are susceptible to lignin removal by mercerization.

The treatments removed hemicelluloses very efficiently, dropping the level from 34 up to 16% by the strongest treatment (NaOH at 10% at 100°C). Hemicelluloses are easily degraded in an alkaline medium (Bufalino et al., 2015). Partially removing highly hydrophilic components

enhances fiber suitability for developing many green materials. For instance, high hemicellulose contents harm cement-based composites by decreasing the fiber-matrix chemical compatibility (César et al., 2019).

The large peak at 3390 cm^{-1} regards O–H stretching (Nascimento et al., 2016). Its sharpening may indicate extractives removal and exposure of cellulose (Bernardes et al., 2023), which happened for all treatments except the mildest one (NaOH at 5% and 80°C). The peak at 2975 cm^{-1} indicates CH_2 asymmetrical stretching of cellulose and hemicelluloses (Bezazi et al., 2014). The more effective removal of hemicelluloses is the feasible explanation for its decrease in the spectra of patauá fibers treated with NaOH at 10% at the two temperatures. Raw *Cocos nucifera* fibers also showed this peak (NagarajaGanesh and Muralikannan, 2016). Wax removal may also change this peak (Karthik and Arunachalam, 2020), indicating the relevance of a higher solvent level. The peak at 2891 cm^{-1} corresponds to the CH_2 symmetric stretching of cellulose and hemicelluloses (Bezazi et al., 2014) and remained similar among the fiber conditions.

The peak at 1658 cm^{-1} regards the C=O stretching vibration of the acetyl in hemicelluloses (Fiore et al., 2014). Its reduction for all treatments, except for the one at 5% NaOH and 80°C, probably regards the partial removal of hemicelluloses and lignin (Karthik and Arunachalam, 2020). The peak at 1592 cm^{-1} indicates C=O of lignin (Amroune et al., 2011) and flattened for all treatments, while the one at 1485 cm^{-1} corresponds to the C=C skeletal vibration of the aromatic lignin (Puglia et al., 2013). The peak at 1186 cm^{-1} that appeared only for the treated fibers relates to the C=O stretching of hemicelluloses (Saaidia et al., 2017). The peak at 1046 cm^{-1} corresponds to the C–O stretching ring of cellulose (Maache et al., 2017). Its height decreased for all treatments, especially for the one carried out with NaOH at 5% and 80°C. The small band at 878 cm^{-1} indicates C-O-C stretching of the β-glycosidic linkage of cellulose (Rosa et al., 2010), and it was similar among all treatments.

Conflicting the chemical composition and FTIR results is crucial to understanding that removing non-cellulosic compounds from the fibers (all treatments achieved in a higher or lower degree) does not necessarily mean similar fiber surfaces. Moreover, while the FTIR overall corroborates the results of hemicelluloses, the lignin peaks appearing or intensifying contrast with the proven removal of this component. The most feasible explanation lies in the lignin occurring at different regions within or between fibers. Lignin in the middle lamella region (primary wall and middle lamella) and in the S2 sublayer of the secondary wall interact differently with the structural carbohydrates (Xu et al., 2020). The proven removal of lignin and fiber individualization supports the lignin degradation in the middle lamella region. Besides a lower temperature, unlike the kraft pulp, mercerization does occur under high pressures. Therefore, the lignin of the secondary wall probably remains in the wall of the fiber, causing the appearance or sharpening of this component's peaks in the FTIR. A previous study also reported increased lignin

intensity on the surface of açaí fibers after alkali treatments (Oliveira et al., 2019). Moreover, a previous work attributed the characteristic absorption band near 780 cm^{-1} to condensed lignin (Fiskari et al., 2016). The appearance of a peak at 800 cm^{-1} in the alkali-treated patauá fibers supports the possibility of a major removal of lignin but its following condensing in the fiber surfaces.

Lignocellulosic fibers are hydrophilic and, under natural conditions, will have moisture. After the thermochemical treatments, clearing pits on the fiber surfaces and partial removal of extractives and lignin possibly made the fibers more susceptible to increased moisture content when kept under the same room conditions as the raw fibers. High moisture contents weaken fiber's mechanical strength and can negatively influence the mechanical strength of composites (Gholampour; Ozbakkaloglu, 2020). Also, moisture can prevent resin curing (Leblon et al., 2013). Therefore, despite improvements in other patauá fiber's attributes for the future development of bioproducts, such as green composites, increased water uptake capacity deserves consideration. Further acetylation and cross-linking are possible alternatives to decrease hydrophobicity again (Sarıoğlu et al., 2023).

Concerning density, both anatomical and chemical changes will affect it. Although the high porosity of treated fibers could decrease their bulk density, the instantaneous immersion methodology for polydisperse material possibly does not capture the void raise effect. Instead, it measures the changes in the cell wall. Therefore, the explanation for the increased density achieved through all treatments lies in thermochemical modifications, specifically the cellulose concentration considering the isolated densities of cellulose (1.528g/cm^3), hemicelluloses (1.52g/cm^3), and lignin (1.30g/cm^3) that make up the fibers (Mussana et al., 2018). Such property enhancement could favor the production of biocomposites and papers of patauá mesocarp fibers.

The natural and alkali-treated fibers could absorb much water, surpassing their own weight with values above 100%. Besides, the more intense the treatment, the higher the water absorption was. Removing the silicon-rich structures from the pits likely made treated fibers more porous, raising their water uptake capability. Additionally, the more hydrophobic lignin was partially removed, and the hydrophilic cellulose was concentrated.

The increase of water absorption is sharper in the first hour but does not stabilize over time. Such a capability is a drawback for composite applications because the fibers swell when they absorb water. If they contract next by losing water, the fiber-matrix interface will weaken. This drawback ultimately reduces the overall mechanical performance of the composites (Thomason et al., 2017). Therefore, applying patauá fibers under any conditions requires proper previous drying up to a moisture content balanced with the environment. On the other hand, fiber high water absorption and swallow loosen microfibrils and favors nanofibrillation by mechanical disintegration (Liu et al., 2019).

CONCLUSIONS

Patauá fibers have unique natural characteristics. They occur as flatted fiber bundles, have silicon-rich structures obstructing their superficial pits, and comprise more lignin than cellulose. When macerated, the fibers are typical and thick-walled. Although patauá is a non-timber resource, the fibers are short-length concerning industrial applications. All alkali treatments caused intense fiber modifications that improve the patauá fibers for bioproduct applications. The temperature was more relevant than the NaOH for most properties, and the 100°C temperature was more effective. However, the recommendation of the NaOH and temperature combination depends on the fiber application. The strongest one (10% of NaOH at 100°C) is recommended for nanofibril production pretreatment based on better fiber individualization, higher cellulose concentration, and increased water absorption capacity. Milder combinations should be selected for composite development because more lignin remains and the water absorptions were lower.

AUTHORSHIP CONTRIBUTION

Project Idea: MCD, TMS, LMM, LB

Funding: MGS, TMS, LMM, LB

Database: OMC, MCD, DNPSO, LCM

Processing: OMC, MCD, DNPSO, LCM

Analysis: OMC, MCD, DNPSO, LCM, LB

Writing: OMC, MCD, DNPSO, MGS, TMS, LCM, LB

Review: MCD, TMS, LMM, LCM, LB

ACKNOWLEDGES

REFERENCES

AJOUGUIM, S.; ABDELOUAHDI, K.; WAQIF, M.; STEFANIDOU, M.; SAÂDI, L. Modifications of Alfa fibers by alkali and hydrothermal treatment. **Cellulose**, v. 26, p. 1503–1516, 2019.

AMROUNE, S.; BEZAZI, A.; BELAADI, A.; ZHU, C.; SCARPA, F.; RAHATEKAR, S.; IMAD, A. Tensile mechanical properties and surface chemical sensitivity of technical fibres from date palm fruit branches (*Phoenix dactylifera* L.). **Composites Part A: Applied Science Manufacture**, v. 71, p. 98-106, 2015.

ASSOCIAÇÃO BRASILEIRA DE NORMAS TÉCNICAS. **MB 1269**: madeira – determinação da densidade básica. Rio de Janeiro, 2003.

ASSOCIAÇÃO BRASILEIRA DE NORMAS TÉCNICAS. **NBR 14929**: madeira – determinação do teor de umidade de cavacos – método por secagem em estufa. Rio de Janeiro, 2017.

ASSOCIAÇÃO BRASILEIRA DE NORMAS TÉCNICAS. **NM 30**: agregado miúdo – determinação da absorção de água. Rio de Janeiro, 2001.

ATTARD, T. M.; CLARK, J. H.; MCELROY, C. R. Recent developments in key biorefinery areas. **Current Opinion in Green and Sustainable Chemistry**, Selected Papers from the 4th Green and Sustainable Chemistry Conference, v. 21, p. 64-74, 2020.

BABÉ, C.; KIDMO, D. K.; TOM, A.; MVONDO, R. R. N.; BOUM, R. B. E.; DJONGYANG, N. Thermomechanical characterization and durability of adobes reinforced with millet waste fibers (*Sorghum bicolor*). **Case Studies in Construction Materials**, v. 13, e00422, 2020.

BALICK, M. J. **Jessenia and Oenocarpus: neotropical oil palms worthy of domestication.** Food and agriculture organization of the United Nations, 1988. 191 p.

BENINI, K. C. C. de C. **Compósitos de nanocelulose/PHBV: manta microfibrilica por eletrofiação.** 2015. 166 f. PhD Thesis Universidade Estadual Paulista, Guaratinguetá, 2015.

BERNARDES, G. P.; ANDRADE, M. P.; POLETTO, M. Effect of alkaline treatment on the thermal stability, degradation kinetics, and thermodynamic parameters of pineapple crown fibres. **Journal of Materials Research and Technology**, v. 23, p. 64-76, 2023.

BEZAZI, A.; BELAADI, A.; BOURCHAK, M.; SCARPA, F.; BOBA, K. Novel extraction techniques, chemical and mechanical characterisation of *Agave americana* L. natural fibres. **Composites Part B: Engineering**, v. 66, p. 194–203, 2014.

BOUSFIELD, G.; MORIN, S.; JACQUET, N.; RICHEL, A. Extraction and refinement of agricultural plant fibers for composites manufacturing. **Comptes Rendus Chimie, v.** 21, n. 9, p. 897-906, 2018.

BRAGA, D. G.; ABREU, J. L. L. de; SILVA, M. G. da; SOUZA, T. M. de; DIAS, M. C.; TONOLI, G. H. D.; OLIVEIRA NETO, C. F. de; CLARO, P. I. C.; GOMES, L. G.; BUFALINO, L. Cellulose nanostructured films from pretreated açaí mesocarp fibers: physical, barrier, and tensile performance. **Cerne**, v. 27, e-102783, 2021.

BROWNING, B. L. **The chemistry of wood**. Interscience Publisher, 1963. 689 p.

BUFALINO, L.; GUIMARÃES, A. A.; SILVA, B. M. da S. e; SOUZA, R. L. F. de; MELO, I. C. N. A. de; OLIVEIRA, D. N. P. S. de; TRUGILHO, P. F. Local variability of yield and physical properties of açaí waste and improvement of its energetic attributes by separation of lignocellulosic fibers and seeds. **Journal of Renewable and Sustainable Energy**, v. 10, n. 5, p. 1-10, 2018.

BUFALINO, L.; SENA NETO, A. R. de; TONOLI, G. H. D.; FONSECA, A. de S.; COSTA, T. G.; MARCONCINI, J. M.; COLODETTE, J. L.; LABORY, C. R. G.; MENDES, L. M. How the chemical nature of Brazilian hardwoods affects nanofibrillation of cellulose fibers and film optical quality. **Cellulose**, v. 22, p. 3657–3672, 2015.

CÉSAR, A. A. da S.; BUFALINO, L.; TAHARA, A. S.; MESQUITA, R. G. de A.; SOUZA, T. M. de; ANDRADE, L. M. F.; MORI, F. A.; MENDES, L. M. Pretreated unbleached cellulose screen reject for cement-bonded fiberboards. **European Journal of Wood and Wood Products**, v. 4, p. 581–591, 2019.

CRUZ, O. M.; SOUZA, R. L. F. de; FREITAS, R. R. de; SOUZA, L. M. de; MAFRA, E. R. M. L. de; SILVA, B. M. da S. e; BUFALINO, L. The properties of the mesocarp fibers of patauá, a multiple-use palm from the Amazonia forest. **SN Applied Sciences**, v. 1, n. 11, p. 1317, 2019.

FIORE, V.; SCALICI, T.; VALENZA, A. Characterization of a new natural fiber from *Arundo donax* L. as potential reinforcement of polymer composites. **Carbohydrate Polymers**, v. 106, p. 77–83, 2014.

FISKARI, J.; DERKACHEVA, O.; KULOMAA, T.; SUKHOV, D. Quick non-destructive analysis of lignin condensation and precipitation by FTIR. **Cellulose Chemistry and Technology**, v. 50, n. 2, p. 213-217, 2016.

FONSECA, A. S.; PANTHAPULAKKAL, S.; KONAR, S. K.; SAIN, M.; BUFALINO, L.; RAABE, J.; MIRANDA, I. P. A.; MARTINS, M. A.; TONOLI, G. H. D. Improving cellulose nanofibrillation of non-wood fiber using alkaline and bleaching pretreatments. **Industrial Crops and Products**, v. 131, p. 203-212, 2019.

FRANKLIN, G. L. Preparation of thin sections of synthetic resins and wood-resin composites, and a new macerating method for wood. **Nature**, v. 155, n. 3924, p. 51-51, 1945.

GHALEHNO, M. D.; KORD, B.; SHESHKAL, B. N. Mechanical and physical properties of wood/polyethylene composite reinforced with TiO_2 nanoparticles. **Cerne**, v. 26, n. 4, p. 474-481, 2020.

GHOLAMPOUR, A.; OZBAKKALOGLU, T. A review of natural fiber composites: Properties, modification and processing techniques, characterization, applications. **Journal of Materials Science**, v. 55, n. 3, p. 829-892.2020.

GROSS, M. How can we save forest biodiversity? **Current Biology,** v. 26, n. 22, p. 1167-1170, 2016.

HASSAN, K.; KANDEEL, E.; KHERALLAH, I.; ABOU-GAZIA, H.; HASSAN, F. *Pinus halepensis* and *Eucalyptus camaldulensis* grown in Egypt: a comparison between stem and branch properties for pulp and paper making. **BioResources**, v. 15, n. 4, p. 7598-7614, 2020.

HENDERSON, A.; GALEANO, G.; BERNAL, R. **Field guide to the palms of the Americas**. Princeton University Press, 1995. 51 p.

INTERNATIONAL ASSOCIATION OF WOOD ANATOMISTS COMMITTEE et al. IAWA list of microscopic features for hardwood identification. **IAWA Bulletin, new series**, v. 10, n. 3, p. 219-332, 1989.

JIN, C.; WU, C.; LIU, P.; YU, H.; YANG, Y.; ZHANG, H. Kinetics of cellulose degradation in bamboo paper. **Nordic Pulp & Paper Research Journal**, v. 37, n. 3, p. 480-488, 2022.

JUNAEDI, H.; BAIG, M.; DAWOOD, A.; ALBAHKALI, E.; ALMAJID, A. Mechanical and physical properties of short carbon fiber and nanofiller-reinforced polypropylene hybrid nanocomposites. **Polymers**, v. 12, 2851, 2020.

KARTHIK, S.; ARUNACHALAM, V. P. Investigation on the tensile and flexural behavior of coconut inflorescence fiber reinforced unsaturated polyester resin composites. **Materials Research Express**, v. 7, 015345, 2020.

KENNEDY, J. F.; PHILLIPS, G. O.; WILLIAMS, E. P. A. **Wood and cellulosics: industrial utilization, biotechnology, structure and properties**. Ellis Horwood, 1987. 1130 p.

LEBLON, B.; ADEDIPE, O.; HANS, G.; HADDADI, A.; TSUCHIKAWA, S.; BURGER, J.; LAROCQUE, A. A review of near-infrared spectroscopy for monitoring moisture content and density of solid wood**. The Forestry Chronicle**, v. 89, n. 5, p. 595-606, 2013.

LI, M.; JIA, Y.; SHEN, X.; SHEN, T.; TAN, Z.; ZHUANG, W.; ZHAO, G.; ZHU, C.; YING, H. Investigation into lignin modified PBAT/thermoplastic starch composites: thermal, mechanical, rheological and water absorption properties. **Industrial Crops and Products**, v. 171, 113916, 2021.

LIU, X.; JIANG, Y.; SONG, X.; QIN, C.; WANG, S.; LI, K. A bio-mechanical process for cellulose nanofiber production – towards a greener and energy conservation solution. **Carbohydrate Polymers**, v. 208, p. 191-199, 2019.

LÖNNBERG, B. Pre-Impregnation of wood chips for alkaline delignification. **Cellulose Chemistry and Technology**, v. 50, n. 5-6, p. 675–680, 2016.

MAACHE, M.; BEZAZI, A.; AMROUNE, S.; SCARPA, F.; DUFRESNE, A. Characterization of a novel natural cellulosic fiber from Juncus effusus L. **Carbohydrate Polymers**, v. 171, p. 163-172, 2017.

MABROUK, A. B.; KADDAMI, H.; BOUFI, S. E.; DUFRESNE, F. Cellulosic nanoparticles from Alfa fibers (*Stipa tenacissima*): extraction procedures and reinforcement potential in polymer nanocomposites. **Cellulose**, v. 19, p. 843–853, 2012.

MORAIS, F. P.; BÉRTOLO, R. A.; CURTO, J. M.; AMARAL, M. E.; CARTA, A. M., EVTYUGIN, D. V. Comparative characterization of eucalyptus fibers and softwood fibers for tissue papers applications. **Materials Letters: X**, v. 4, p. 100028, 2019.

MULINARI, D. R. Compósitos de poliuretano reforçados com fibra de sisal. **Cadernos UniFOA**, v. 9 n. 1, p. 65-71, 2014.

MUSSANA, H.; YANG, X.; TESSIMA, M.; HAN, F.; IQBAL, N.; LIU, L. Preparation of lignocellulose aerogels from cotton stalks in the ionic liquid-based co-solvent system. **Industrial Crops and Products**, v. 113, p. 225-233, 2018.

NAGARAJAGANESH, B.; REKHA, B. Intrinsic cellulosic fiber architecture and their effect on the mechanical properties of hybrid composites. **Archives of Civil and Mechanical Engineering**, v. 20, 125, 2020.

NASCIMENTO, P.; MARIM, R.; CARVALHO, G.; MALI, S. Nanocellulose produced from rice hulls and its effect on the properties of biodegradable starch films. **Material Research**, v. 19, n. 1, p. 167–174, 2016.

NASSAR, M. M. A.; ALZEBDEH, K. I.; AL-HINAI, N.; PERVEZ, T. A new multistep chemical treatment method for high-performance natural fibers extraction. **Journal of Natural Fibers**, v. 20, 2150922, 2023.

NOORI, A.; LU, Y.; SAFFARI, P.; LIU, J.; KE, J. The effect of mercerization on thermal and mechanical properties of bamboo fibers as a biocomposite material: a review. **Construction and Building Materials**, v. 297, 122519, 2021.

OLIVEIRA, D. N. P. S. de; CLARO, P. I. C.; FREITAS, R. R. de; MARTINS, M. A.; SOUZA, T. M.; SILVA, B. M. da S.; MENDES, L. M.; BUFALINO, L. Enhancement of the amazonian açaí waste fibers through variations of alkali pretreatment parameters. **Chemistry & Biodiversity**, v. 16, n. 9, p. 1-12. 2019.

PUGLIA, D.; MONTI, M.; SANTULLI, C.; SARASINI, F.; ROSA, I. M. DE; KENNY, J. M. Effect of alkali and silane treatments on mechanical and thermal behavior of *Phormium tenax* fibers. **Fibers and Polymers**, v. 14, p. 423-427, 2013.

ROSA, I. M.; KENNY, J. M.; PUGLIA, D.; SANTULLI, C.; SARASINI, F. Morphological, thermal and mechanical characterization of okra (*Abelmoschus esculentus*) fibres as potential reinforcement in polymer composites. **Composites Science Technology**, v. 70, p. 116–22, 2010.

SAAIDIA, A.; BEZAZI, A.; BELBEH, A.; BOUCHELAGHEM, H.; SCARPA, F.; AMIROUCHE, S. Mechano-physical properties and statistical design of jute yarns. **Measurement**, v. 111, p. 284-294, 2017.

SARIOĞLU, E.; TURHAN, E. A.; KARAZ, S.; BENGÜ, B.; BIÇER, A.; YARICI, T.; ERKEY, C.; SENSES, E. A facile method for cross-linking of methacrylated wood fibers for engineered wood composites. **Industrial Crops and Products**, v. 193, 116296, 2023.

SILVA, R. V. da. **Compósito de resina poliuretano derivada de óleo de mamona e fibra vegetais**. 2003. 157 p. PhD thesis Universidade de São Paulo, São Carlos.

SIMELANE, S.P.; MADYIRA, D.M. Effect of mercerization on coconut fiber surface condition for use in natural fiber-reinforced polymer composites. In: VON LEIPZIG, K.; SACKS, N.; MC CLELLAND, M. **Smart, sustainable manufacturing in an ever-changing world**. Springer, 2023. p. 701-716.

TECHNICAL ASSOCIATION OF THE PULP AND PAPER ASSOCIATION. **TAPPI T 413 om-17**: ash in wood, pulp, paper and paperboard: combustion at 900°C. Peachtree Corners, 2016.

TECHNICAL ASSOCIATION OF THE PULP AND PAPER ASSOCIATION. **TAPPI T 204 cm-17**: solvent extractives of wood and pulp. Peachtree Corners, 2017.

TECHNICAL ASSOCIATION OF THE PULP AND PAPER INDUSTRY. **TAPPI T 222:** acid-insoluble lignin in wood and pulp**.** Peachtree Corners, 2015.

TECHNICAL ASSOCIATION OF THE PULP AND PAPER INDUSTRY. **TAPPI UM 250:** acid-soluble lignin in wood and pulp**.** Peachtree Corners, 2000.

THOMASON, J; YANG, L; GENTLES, F. Characterisation of the anisotropic thermoelastic properties of natural fibres for composite reinforcement. **Fibers**, v. 5, n. 4, p. 1-2, 2017.

VIVIAN, M. A; MODES, K. S; CAETANO, A. P. Potencial da madeira de *Pinus glabra* para produção de polpa celulósica. **Madera y Bosques**, v. 26, n. 3, 2020.

XU, E.; WANG, D.; LIN, L. Chemical structure and mechanical properties of wood cell walls treated with acid and alkali solution. **Forests**, v. 11, n. 87, 2020.

WHEELER, E. A.; BAAS, P. A survey of the fossil record for Dicotyledonous wood and its significance for evolutionary and ecological wood anatomy. **IAWA Journal**, v. 12, p. 275–318, 1991.

ZAKIKHANI, P.; ZAHARI, R.; SULTAN, M. T. H.; MAJID, D. L. Extraction and preparation of bamboo fibre-reinforced composites. **Materials & Design**, v. 63, p. 820-828, 2014.